Isoelectronically substituted heavy-fermion compounds $CeCu_{6-x}Au_x$, studied by local probe and electronic band structure calculation

M. Winkelmann, G. Fischer, and B. Pilawa
Physikalisches Institut, Universität Karlsruhe, D-76128 Karlsruhe, Germany

M. S. S. Brooks
Commission of the European Communities, Joint Research Center, Institute for Transuranium Elements, D-76021 Karlsruhe, Germany

E. Dormann
Physikalisches Institut, Universität Karlsruhe, D-76128 Karlsruhe, Germany

(Received 21 December 2005; revised manuscript received 13 February 2006; published 7 April 2006)

For $CeCu_{6-x}Au_x$ ($x=0,0.1,1$), we measured the temperature dependence of $^{63,65}Cu$ nuclear magnetic resonance spectra of oriented single-crystal powder at 7 T in the 5–100 K range. Ce^{3+} crystal field and molecular field parameters are derived from single-crystal magnetic susceptibility data. Calculated electric field gradients are used to correctly assign nuclear quadrupole resonance frequencies to lattice sites (n). Bare Knight shifts and transferred hyperfine interaction coupling constants $\alpha(n)$ as well as electric field gradient information are extracted for the various Cu sites (n). *Ab initio* self-consistent energy-band calculations explain the electric field gradients and the alternation of the sign of $\alpha(n)$. The anisotropy of the hyperfine coupling parameter α is proved for the a-c plane for the Cu(5) site.

DOI: 10.1103/PhysRevB.73.165107 PACS number(s): 71.27.+a, 76.60.Cq, 75.20.Hr

I. INTRODUCTION

The pseudobinary intermetallic compounds $CeCu_{6-x}Au_x$ received considerable interest in recent years:[1] $CeCu_6$ is one of the best-known heavy-fermion paramagnets with no magnetic order above the milli-Kelvin range, the isoelectronic structurally ordered compound $CeCu_5Au$ is a heavy-fermion antiferromagnet with $T_N=2.3$ K, and for $x\approx 0.1$ signatures of non-Fermi liquid behavior were reported.[2] Nevertheless, the interplay between Kondo-like shielding of the Cerium $4f$ moment having a $^2F_{5/2}$ Hund's rule ground state with Ising-like low-temperature magnetic anisotropy,[3] and the antiferromagnetic long-range coupling [supposedly of Ruderman-Kittel-Kasuya-Yosida- (RKKY-) like origin[4]] actually is not really understood.

In principle, nuclear magnetic resonance (NMR) is a rather useful tool for the study of static and dynamic properties of conduction electron polarization in a heavy-fermion compound. However, Cu NMR spectra of $CeCu_6$ or $CeCu_5Au$ in external magnetic fields tend to be extremely confusing because the spectra of both isotopes ^{63}Cu and ^{65}Cu ($I=3/2$, $Q\neq 0$, Table I) are split by quadrupolar interaction by more than 20 MHz and overlap almost entirely. Furthermore, the unit cell contains four formula units (28 atoms) with five (six) crystallographically inequivalent Cu sites in the orthorhombic high- (or the monoclinic low-) temperature phase of $CeCu_6$ (Fig. 1), and still with four inequivalent Cu sites in the ternary compound $CeCu_5Au$.[8,9] Since the symmetry of these sites allows for fully developed anisotropy of the magnetic hyperfine and the electric quadrupolar interaction, up to 108 NMR lines or powder-pattern edge singularities may be expected for $^{63,65}Cu$ high-field powder-sample NMR. Thus, except for some early NMR attempts,[10–12] only nuclear quadrupole resonance (NQR) was applied to the heavy-fermion compounds $CeCu_{6-x}Au_x$,[13–19] reducing the variety thus to about ten partially overlapping NQR lines (without the erroneously assumed "zero-frequency" line[13]). Unfortunately, however, conduction electron spin polarization can not be unraveled in this way.

We report an analysis of the electronic structure of $CeCu_{6-x}Au_x$ by combination of electronic-band structure calculation and nuclear magnetic resonance. Electric field gradients are calculated for $CeCu_6$ and $CeCu_5Au$ using the Wien program package[20–22] in order to assign electric field gradients to lattice sites, as an extension of the early, unfortunately misleading, attempts based on the simple point charge model.[13] $^{63,65}Cu$-NMR measurement in 7 T external field, using powdered single crystals, oriented at low temperature via their large magnetic anisotropy, supply the magnetic hyperfine field, transferred from Ce^{3+} to Cu neighbors as local probes. By measurement of the NMR line shifts and the single-crystal static magnetic susceptibility and by calculation of the Ce susceptibility subject to crystal field, exchange and Kondo effect in dependence of temperature, and by the correlation of these quantities with the temperature as an implicit parameter, known as Jaccarino-Clogston plot,[5] i.e.,

TABLE I. NMR parameters of the two Cu isotopes (Refs. 5–7).

Isotope	^{63}Cu	^{65}Cu	Ratio 63/65
Abundancy	69.1%	30.9%	2.24
I	3/2	3/2	1
$\gamma/2\pi$ (MHz/T)	11.285	12.090	0.933
$Q(10^{-31}$ m$^2)$	−220 (15)	−204 (14), 195(4)	1.078, 1.128[a]

[a]In the present investigation, the ratio 1.081(3) is observed.

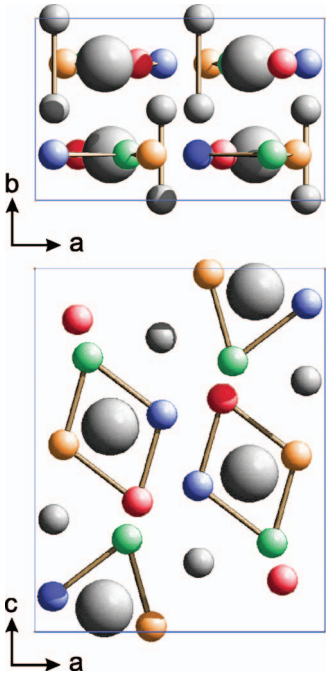

FIG. 1. (Color) Orthorhombic crystal structure of $CeCu_6$ (Ref. 8) seen against c direction (top) and along b direction (bottom). Ce: large gray spheres; Cu(1,6): gray; Cu(2): red; Cu(3): green; Cu(4): blue; Cu(5): yellow. The shortest Cu-Cu separations are indicated by lines. The shortest average Cu-Ce separation occur for Cu(4) and Cu(5). Only the Cu(1) sites shift at the Pnma$\rightarrow$P2$_1$/c transition. For $CeCu_5Au$ the Cu(2) site is occupied by Au. For simplicity, we use the orthorhombic $CeCu_6$ site designation and the color code defined in this figure throughout this contribution.

$$\frac{\Delta\nu(T)}{\nu_0} = K_{0,i} + \alpha_i \frac{\chi_i^{\mathrm{mol}}(T)}{N_A}, \tag{1}$$

the site-dependent (n) Knight shift $K_{0,i}(n)$ and the respective transferred hyperfine field coupling constant $\alpha_i(n)$ are obtained for a well-defined orientation (i). The coupling constant α can be decomposed into two parts:

$$\alpha_i(n) = \alpha_i^{\mathrm{dip}}(n) + \alpha_i^{\mathrm{THF}}(n). \tag{2}$$

The field-parallel component of the classical dipolar field α_i^{dip}, which is due to the field-dependent total electronic moments of all Cerium ions in the $CeCu_{6-x}Au_x$ compound, can easily be calculated[6] for the known crystal structure, approximated here by the high-temperature orthorhombic structures.[8,9]

The second contribution, $\alpha_i^{\mathrm{THF}}(n)$, yields information about the electronic structure and exchange coupling in the respective intermetallic compound.[5] The RKKY model would be the simplest approximate model for the calculation of $\alpha^{\mathrm{THF}}(n)$. In this model,[4] the conduction electrons are polarized at the Ce^{3+} sites by local $4f$-spin conduction-electron spin-exchange interaction and their spatially oscillating, slowly with distance decaying polarization, is summed up at the Cu site in question and is felt by hyperfine interaction of these polarized conduction electrons with the ^{63,65}Cu nucleus.[5] Reality is generally more complicated, and for dense magnetic systems like the RCu_6 intermetallic compounds, the nearest magnetic neighbors of the nonmagnetic Cu site tend to predominate compared to all other, possibly oscillating long-distance contributions, yielding—inspite of their small number—typically, 50–80% of the total transferred field.[23,24,5] Furthermore, it has been shown that a more complicated Hamiltonian is required and appropriate for the description of the exchange interaction of the Ce^{3+}-$4f^1$-electron with crystal field split $J=5/2$ levels in the metallic matrix, giving rise—besides others—to anisotropic interactions.[25,26] The NMR analysis of the hyperfine interaction, reported below for all Cu sites in the antiferromagnet $CeCu_5Au$, the paramagnet $CeCu_6$ and the "non-Fermi liquid" system $CeCu_{5.9}Au_{0.1}$, allows one to discover such perculiarities of the electronic structure. This will be exploited in this contribution.

The questions raised here can only be analyzed experimentally by applying an external magnetic field to the sample, and not by using the nuclear quadrupole resonance in zero external field. We show that NMR of $CeCu_5Au$ or $CeCu_6$ powder samples in large external magnetic field can be used and analyzed, in spite of the expected confusions alluded to above.[6,27–30] This is rendered possible by powder grain orientation caused by the large magnetic anisotropy at low temperatures. In contrast to our earlier less successful attempts, single crystals were powdered for the current investigations because this allows for a uniform orientation of each powder grain. Otherwise, in spite of the preferential orientation of the grains with their Ising-like c direction parallel to the external field, minority portions of the same polycrystalline grains evidently were oriented also with arbitrary direction parallel to the external field. This turned out to be a severe obstacle to unequivocal data analysis.[6,28] Care has to be taken for the extraordinary variety of anisotropies, nevertheless, because the main axes of the electric field gradient tensors of the various Cu sites are inclined by different angles with respect to the axes of the orthorhombic unit cell.

Our paper is organized as follows. In Sec. II, we describe the experimental conditions, and in Sec. III, we present representative experimental results. We start the discussion of the results, Sec. IV, with the explanation of our single-ion crystal field and *ab initio* self-consistent energy-band calculations (Sec. IV A). In Sec. IV B, the electric field gradients at the Cu sites and their role for the site assignment are discussed. Section IV C is devoted to the trends of the hyperfine coupling constants within the $CeCu_{6-x}Au_x$ series. Summarizing conclusions are extracted in Sec. V.

II. EXPERIMENTAL CONDITIONS

The growth of $CeCu_{6-x}Au_x$ single crystals by the Czochralski method has already been described.[2,9] The magnetic susceptibility for the three main crystallographic axes of single crystals has been determined with a Quantum Design MPMS SQUID (superconducting quantum interference device) magnetometer (Fig. 2). For the NQR and NMR measurements with a Bruker MSL 300 spectrometer the samples were powdered and sealed in a quartz glass (suprasil) ampoule.[27–31,6] NQR quadrupolar echos were excited by two

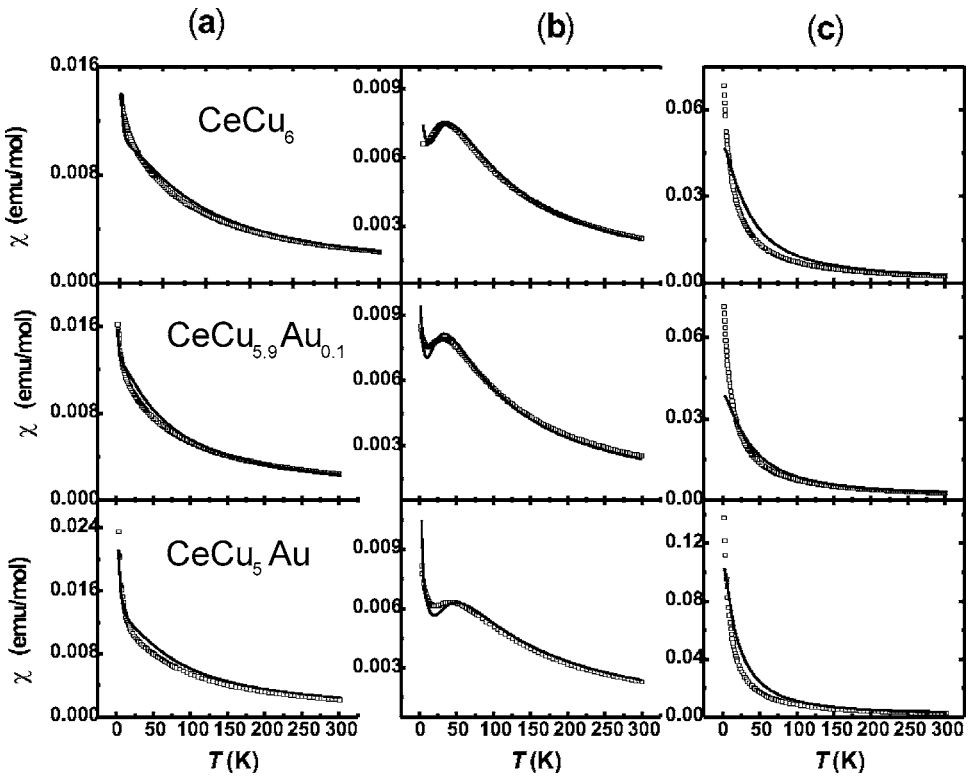

FIG. 2. Molar magnetic susceptibility of $CeCu_{6-x}Au_x$ single crystals for external magnetic field $B_0=5$ T along the crystallographic main axes a,b,c for $x=0$, 0.1, and 1.0. The solid line fits are explained in Sec. IV A 1. The fit parameters are given in Table III.

90° pulses of 2 μs length, NMR spin echos by a 90°–180° pulse sequence with pulse lengths of 2 and 4 μs, respectively. Appropriate phase cycling was adopted for the NQR as well as NMR measurements. Only NMR spin-echo spectra recorded at fixed field of 7 T, variable temperature, for samples first oriented by high field at low temperature are presented. Since only the line positions were of interest, spectra were obtained in 50 kHz steps by Fourier transformation of the second half of the spin echo and integration over ±25 kHz, without correction for relaxation or excitation and detection conditions (Fig. 3). Thus the relative signal amplitudes for a wider frequency range can not be compared quantitatively.

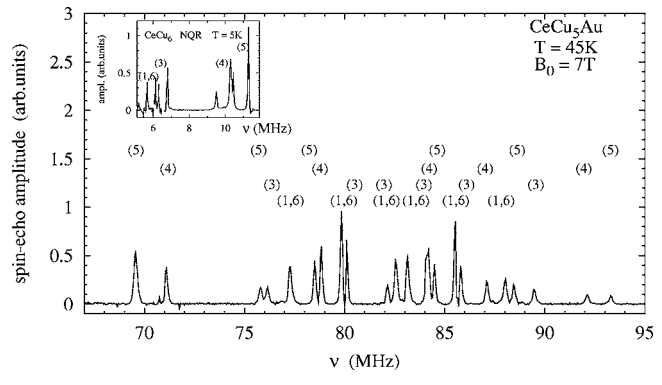

FIG. 3. Uncalibrated NMR spin-echo Fourier transform spectrum of $CeCu_5Au$ oriented single-crystal powder sample vs frequency ($B_0=7$ T, $T=45$ K) excited by two pulses of 2 μs and 4 μs duration and 50 μs separation. Site assignment is indicated. The inset shows part of the $CeCu_6$ NQR spectrum at 5 K as an example.

III. RESULTS

A. Static magnetic susceptibility

For $CeCu_6$, earlier single-crystal measurements indicated for the high-temperature range $T>100$ K effective Ce^{3+} moments of $\mu_{\text{eff}}=2.60\mu_B$, $2.63\mu_B$, and $2.49\mu_B$, and asymptotic Curie temperatures $\theta_p=-54$ K, -70 K, and -8 K for the a, b, and c axis, respectively.[32] These experimental data could be reproduced approximately by consideration of the orthorhombic crystal field and an antiferromagnetic molecular field $[\lambda=25\ (\text{emu/mol})^{-1}]$.[33] From our measurements of $CeCu_6$ single crystals,[30] we derive $\mu_{\text{eff}}=(2.61\pm0.12)\mu_B$, $(2.67\pm0.08)\mu_B$, and $(2.44\pm0.06)\mu_B$, and $\theta_p=-(69.9\pm0.5)$ K, $-(65.1\pm0.3)$ K, and $-(2.6\pm0.1)$ K for the a, b, and c axes, respectively.

Figure 2 shows our results for the a-, b-, and c-axis magnetic susceptibility for $CeCu_{6-x}Au_x$ ($x=0$, 0.1, and 1.0). For the subsequent NMR analysis, the relative variation in the low-temperature range 5–100 K is of primary interest. The c-axis susceptibility χ_c is the largest one for all concentrations x, $0\leqslant x\leqslant 1$, in this temperature range, and increases continuously with decreasing temperature. For temperatures above 50 K, χ_a and χ_b are not different enough to allow the discrimination of a single-crystal grain's orientation based on susceptibility measurement, both are significantly smaller than χ_c, however. For temperatures below 50 K, χ_b is almost constant and clearly smaller than χ_a, which continues to increase with decreasing temperature. Thus, the T-dependent behavior in this low-temperature range allows one to identify a single-crystal grain's orientation from χ_{rel} vs T analysis, unambiguously.

TABLE II. Electric field gradients (calculated) and NQR frequencies [calculated or measured (Refs. 13, 14, and 19)] at Cu sites in $CeCu_{6-x}Au_x$, with orthorhombic site designation of $CeCu_6$. In brackets, the data for ^{197}Au on the Cu(2) site are given for $CeCu_5Au$.

	x	Cu(1,6)	Cu(2)	Cu(3)	Cu(4)	Cu(5)
Calculated: eq(10^{21} V/m^2)	0	−1.94	−0.90	−2.70	−3.69	−4.11
	1	−1.56	(−4.80)	−2.52	−3.85	−4.49
η	0	0.67	0.73	0.23	0.53	0.45
	1	0.67	(0.20)	0.17	0.46	0.14
$\nu_{NQR}(^{63/65}Cu)$ (MHz)	0	5.53/5.13	2.60/2.41	7.24/6.72	10.26/9.52	11.29/10.48
	1	4.45/4.13	(31.95)	6.73/6.25	10.59/9.83	11.98/11.11
Measured $\nu_{NQR}(^{63/65}Cu)$ (MHz)	0	6.08/5.63	3.91/3.61	6.81/6.32	10.35/9.57	11.33/10.52

B. NQR spectra

Some of the already published lines of $CeCu_{6-x}Au_x$ samples ($x=0$, 0.1, and 1) were verified at 5 K in zero external field, for nonoriented single-crystal powder samples. The substantial broadening of the lowest NQR lines due to inappropriate sample preparation[14] and of the highest frequency line for $x\neq 0$ was demonstrated already by other investigations.[19] The comparably small width of the NQR lines recorded here supports the good quality of our powdered single-crystal samples. The pairs of lines originating from the two isotopes ^{63}Cu and ^{65}Cu on the same crystallographic site, Cu(n), can easily be discriminated based on their 2.2:1 abundance and 1.08:1 frequency ratio. For the Cu(1,6) sites, a line splitting is observed in $CeCu_6$ due to its monoclinic low-temperature distortion (i.e., 6.06–6.12 MHz/5.62–5.68 MHz). The line splitting amounts to about 59/53 kHz and is thus only barely resolved. For the ease of comparison to the calculated NQR frequencies allowing the site assignment, all known peak frequencies for $CeCu_6$ are given in Table II.

C. NMR spectra

Figure 3 shows a typical fixed field, fixed temperature, variable frequency Cu-NMR spectrum of an oriented single-crystal powder sample of $CeCu_{6-x}Au_x$, in this case for $x=1.0$, $T=45$ K and $B_0=7$ T. It is evidently highly structured, but, nevertheless, rather confusing. A certain degree of line clustering or centering around the bare Zeeman frequencies of $\nu_{0,z}=79.55$ MHz (85.22 MHz) for ^{63}Cu (^{65}Cu) can be observed, however. Intuition is better supported by a plot of the respective line positions vs temperature, as is visualized by Fig. 4. These data give direct evidence for the distinction between central lines or quadrupole satellites and between positive or negative transferred hyperfine field coupling constants $\alpha_c(n)$ via the direction of the paramagnetic line shifts toward high or low frequency. Line shifts by more than 2 MHz (or 2.5%) are observed for temperature variation between 5 and 100 K. Further analysis of these line positions and shifts is discussed in Secs. IV B and IV C.

IV. DISCUSSION OF THE RESULTS

A. Numerical results

1. Crystal field effects and exchange interactions

In $CeCu_{6-x}Au_x$, the Ce^{3+}-$4f^1$-$^2F_{5/2}$ ground state is split by the orthorhombic or monoclinic crystal field into three doublets (at energies 0, E_1, and E_2). The lowest-lying doublet is built up to more than 90% from the $|M=\pm 5/2\rangle$ wave function and for the first excited doublet (according to neutron scattering at $E_1=7-8.6$ meV or 80–100 K),[34] the $|\pm 3/2\rangle$ functions predominate. For $CeCu_6$ and $CeCu_{5.5}Au_{0.5}$, the crystal field splitting is known from neutron scattering.[34] A calculation of the crystal field dominated low-temperature single-ion magnetic susceptibility (and its anisotropy) requires the adjustment of five crystal field parameters. No improvement of the agreement for all orientations could be

TABLE III. Crystal field and molecular field parameters for Ce^{3+} in $CeCu_{6-x}Au_x$. $(E_2-E_1)=5.75$ meV was used independent of x.

x	0	0.1	1.0
E_1 (meV)	6.0±0.1	4.6±0.1	7.2±0.1
B_2^0 (K)	−6.776±0.191	−5.710±0.099	−7.488±0.121
B_2^2 (K)	+1.247±1.000	+0.924±0.504	−1.492±1.187
B_4^0 (K)	+0.0274±0.030	+0.048±0.015	+0.046±0.015
B_4^2 (K)	−0.678±0.094	−0.750±0.045	−0.694±0.117
B_4^4 (K)	−0.339±0.062	−0.312±0.036	−0.478±0.092
λ [(emu/mol)$^{-1}$]	17.4±0.2	22.0±0.2	5.6±0.2

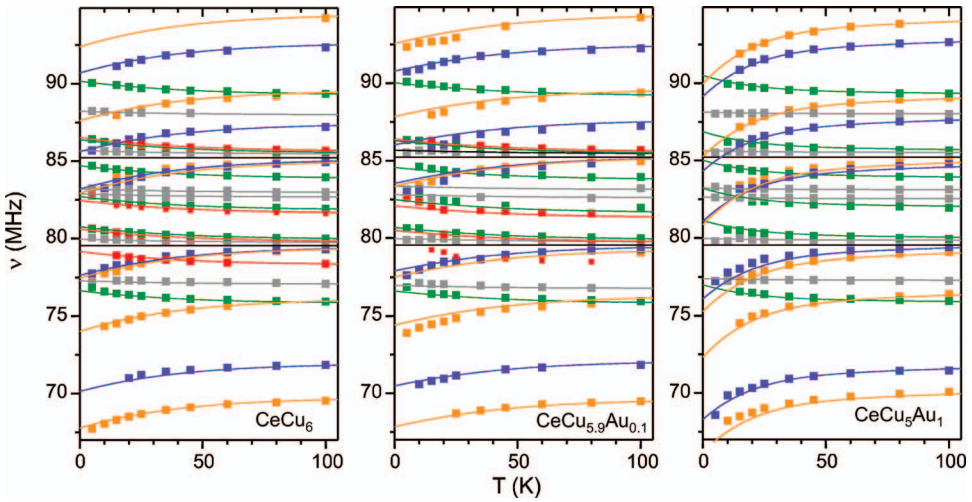

FIG. 4. (Color) Cu-NMR line positions versus temperature for ^{63}Cu and ^{65}Cu in $CeCu_{6-x}Au_x$ ($x=0,0.1,1$), ($B_0=7$ T). The straight solid lines indicate the bare Zeeman frequencies according to the gyromagnetic ratios compiled in Table I. The color code of the assigned crystallographic sites is defined in Fig. 1. The solid lines show the fit explained in Sec. IV C.

achieved when a deviation of the preferred crystal field axis by plus or minus θ from the c axis in the a-c plane was considered, inspite of this being allowed by the low site symmetry of the four Ce sites in the unit cell.[35] As a further approximation, the Kondo-like shielding and the influence of spin and orbit exchange scattering on the mutual interaction of the Ce moments is described by just one antiferromagnetic molecular field constant λ, as before,[33] i.e.,

$$\chi_i^{\mathrm{cal}}(T) = \frac{\chi_i^{si}(T)}{1+\lambda\chi_i^{si}(T)}, i=a,b,c. \tag{3}$$

The adjusted parameters are compiled in Table III. Figure 2 shows the perfect agreement between the temperature dependence of the experimentally observed single-crystal magnetic susceptibility, χ_i^{mol}, for the orthorhombic a and b direction parallel to the magnetic field, and the respective calculated intrinsic variation (solid lines). The largest deviation is observed for the preferred c direction in the temperature range around 50 K, indicating that the approximation of a temperature-independent λ value might not be fully justified. It is important to note that the largest low-temperature values of $\chi_c(T)$ are observed for the compound with $x=1$, in spite of the fact that this compound actually orders antiferromagnetically below $T_N=2.3$ K (Fig. 2). This is reflected by the smallest antiferromagnetic molecular field constant λ appropriate for $x=1$ in Eq. (3) (Table III). This indicates that Kondo-like shielding of the Ce^{3+} moment is weaker for $x=1$ than for $x=0$.

2. Electric field gradients (EFGs)

The electric field gradient tensors at the various Cu sites in $CeCu_6$ and $CeCu_5Au$ (i.e., $x=0$ and 1) were calculated with use of the WIEN2K program package.[20,21] Relevant data are reproduced in Table II. The NQR frequency is obtained as[36]

$$\nu_{\mathrm{NQR}} = \nu_Q\left(1+\frac{\eta^2}{3}\right)^{1/2} \tag{4}$$

for $I=3/2$, with $\nu_Q=e^2qQ/2h$ and with the experimental values of Q for the two isotopes ^{63}Cu and ^{65}Cu given in Table I. As usual, $\mathrm{eq}\equiv V_{zz}$, $\eta=\frac{V_{xx}-V_{yy}}{V_{zz}}$, and $V_{xx}+V_{yy}+V_{zz}=0$. The comparison of the calculated and measured NQR frequencies in Table II shows the excellent agreement and leaves no doubt concerning the assignment of crystallographic sites and NQR frequencies. The point charge model used for the

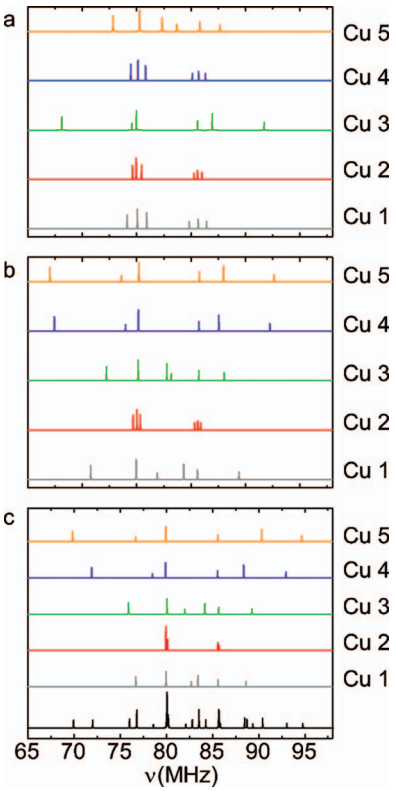

FIG. 5. (Color) Calculated NMR spectra of the five crystallographically inequivalent Cu sites in $CeCu_6$ (orthorhombic structure) for both isotopes, ^{63}Cu and ^{65}Cu, and for magnetic field of 7 T along the crystallographic a, b, or c direction (Knight and paramagnetic shift neglected). Color code is defined in Fig. 1. For c orientation, the lowest trace shows also the resulting superimposed spectrum. Note that the frequency range is 65–98 MHz for c-orientation, but 70–98 MHz for a- and b-orientation.

TABLE IV. Knight shifts in $CeCu_{6-x}Au_x$ for the inequivalent Cu sites (orthorhombic denotation of $CeCu_6$) for magnetic field in c direction, $K_{0,c}$, in percent. (The error bar takes also the difference between calculated and measured $\chi_c(T)$ into account.)

	$CeCu_6$	$CeCu_{5.9}Au_{0.1}$	$CeCu_5Au$
Cu(1,6)	+0.275(24)	+0.223(62)	+0.383(8)
Cu(2)	+0.327(51)	+0.305(116)	
Cu(3)	+0.258(66)	+0.222(120)	+0.409(52)
Cu(4)	+0.250(108)	+0.242(195)	−0.097(214)
Cu(5)	+0.184(136)	+0.209(178)	−0.011(115)
Average	+0.262(80)	+0.237(132)	+0.213(111)

earlier tentative assignment, thus, evidently was misleading.[13]

Figure 5 shows the calculated quadrupolar splitted NMR spectra of ^{63}Cu and ^{65}Cu (exact diagonalization) for the orthorhombic high-temperature structure of $CeCu_6$, for magnetic field of 7 T parallel to the c direction and for neglected Knight and paramagnetic shift for the various Cu sites. This allows for an unequivocal assignment of Cu sites and observed NMR lines. For the quantitative analysis of the NMR spectra, for each site, the three NMR lines of each isotope can be calculated, approximately, for given orientation of the external magnetic field with respect to the local magnetic axes (θ, ϕ) and with respect to the local electric field gradient main axes (ϑ, φ) according to[36,37]

$$\nu_c = \nu_z + \Delta\nu^{(2)}_{Q_{1/2}} \tag{5}$$

for the central line $(+1/2 \leftrightarrow -1/2$ transition) and

$$\nu_{H,L} = \nu_z + \Delta\nu^{(2)}_{Q_{3/2}} \pm \Delta\nu_Q \tag{6}$$

for the high (H) and low (L) frequency quadrupole satellites, or $+1/2 \leftrightarrow +3/2$, and $-3/2 \leftrightarrow -1/2$ transitions, respectively. Here,

$$\nu_z = \nu_{0,z}[1 + K_0(\theta,\phi) + \alpha(\theta,\phi)\chi^{mol}_{\theta,\phi}(T)], \tag{7}$$

with $\nu_{0,z} = (\gamma_0/2\pi)B_0$,

$$\Delta\nu_Q = \tfrac{1}{2}\nu_Q[3\cos^2\vartheta - 1 - \eta\sin^2\vartheta\cos(2\varphi)], \tag{8}$$

and

$$\Delta\nu^{(2)}_{Q_{1/2}} = -\frac{3\nu_Q^2}{16\nu_z}(1-\cos^2\vartheta)\left\{9\left[1+\frac{2}{3}\eta\cos(2\varphi)\right]\cos^2\vartheta - \left[1-\frac{2}{3}\eta\cos(2\varphi)\right]\right\} - \frac{3\eta^2}{72}\frac{\nu_Q^2}{\nu_z} \times\left[4-\cos^2\vartheta+\frac{27}{16}\cos^2(2\varphi)(1-\cos^2\vartheta)^2\right] \tag{9}$$

$$\Delta\nu^{(2)}_{Q_{3/2}} = +\frac{3}{2}\frac{\nu_Q^2}{\nu_z}(1-\cos^2\vartheta)\left[1+\frac{2}{3}\eta\cos(2\varphi)\right]\cos^2\vartheta + \frac{3\eta^2}{72}\frac{\nu_Q^2}{\nu_z}\left[4-9\cos^2\vartheta-\frac{109}{16}\cos^2(2\varphi)(1-\cos^2\vartheta)^2\right] \tag{10}$$

For the present analysis, however, numerical diagonalization was used. Equations (1) and (7) define the most relevant parameters accessible from the analysis of the NMR spectra of the oriented single-crystal powder samples that will be discussed below: the Knight shifts for c orientation, $K_{0,c}(n)$ (see Table IV), and the transferred hyperfine field coupling constants, $\alpha_c(n)$ (see Table V) of the different Cu sites, Cu(n), the latter being related to the experimental magnetic susceptibility, $\chi^{mol}_c(T)$.

3. Conduction electron polarization

As reported earlier,[6] the RKKY model does not explain the observed alternation of the sign of the transferred hyperfine field coupling constants $\alpha_i^{THF}(n)$ of paramagnetic $CeCu_6$. It is possible to estimate the transferred hyperfine fields if the partial magnetic moments at the Cu sites induced by a Ce $4f$ spin can be calculated. This can be done in a self-consistent energy-band calculation in which the Ce $4f$ spin is constrained to a given value provided that the induced moments are proportional to the Ce $4f$ spin. The model we have in mind is that an applied field induces mainly Ce $4f$ moments since the $4f$ susceptibility is far higher than the conduction electron susceptibility. The Ce $4f$ spins then polarize the conduction electrons at the Ce sites through local exchange interactions. Hybridization between the Ce and Cu conduction electrons then leads to an induced spin polarization at the Cu sites.

A series of self-consistent spin polarized energy band calculations were therefore carried out using the linear-muffin-tin-orbital (LMTO) method[38,39] in the atomic sphere approximation (ASA) with potentials obtained from the local-spin-density approximation[40] (LSDA) to density functional theory[41,42] with values of Ce $4f$ spin varying from 0.25 to $1.0\mu_B$. The method used to constrain the Ce $4f$ spin is described in Ref. 43. Four formula units in the high-temperature orthorhombic structure of $CeCu_6$ (Pnma, a =0.81088, b=0.51004, c=1.01621 nm) were taken into ac-

TABLE V. Transferred hyperfine field coupling constants in $CeCu_{6-x}Au_x$ for the inequivalent Cu sites (orthorhombic denotation) and magnetic field in the c direction observed from fit to 5–100 K data. α^{dip} calculated for $CeCu_6$ structure. α_a is derived for a polycrystalline powder sample in Ref. 6. [The error bar takes also the difference between calculated and measured $\chi_c(T)$ into account.]

	α_c^{exp} (kOe/μ_B)			α_c^{dip} (kOe/μ_B)	α_c^{THF} (kOe/μ_B)		
Site	$x=0$	0.1	1.0		$x=0$	0.1	1.0
Cu(1,6)	+0.34(11)	+0.40(26)	+0.07(6)	+0.29	+0.05(11)	+0.11(26)	−0.22(6)
Cu(2)	+1.34(22)	+1.53(39)		+0.30	+1.04(22)	+1.23(39)	
Cu(3)	+1.31(13)	+1.57(42)	+0.73(18)	+0.46	+0.85(13)	+1.11(42)	+0.27(18)
Cu(4)	−2.92(33)	−3.20(69)	−2.22(44)	−0.58	−2.34(33)	−2.62(69)	−1.64(44)
Cu(5)	−3.18(39)	−3.52(73)	−2.54(49)	−0.78	−2.40(39)	−2.74(79)	−1.76(48)
	α_a^{exp} (kOe/μ_B)			α_a^{dip} (kOe/μ_B)	α_a^{THF} (kOe/μ_B)		
Site	$x=0$	0.1	1.0		$x=0$	0.1	1.0
Cu(5)	+2.48(34)			+0.26	+2.22(34)		

count. The induced moments at all were found to be approximately proportional to the Ce $4f$ spin.

The results for the calculation with the cerium $4f$ magnetic moment fixed to $1\mu_B$ are shown in Table VI. The partial s, p, and d moments for the various sites (μ_s, μ_p, μ_d) as well as the respective sums of partial spin-up plus spin-down moments per site (n_s, n_p, n_d) are shown. The last column presents the estimated isotropic hyperfine coupling constants $\alpha(n)$ calculated with the simplified relation[5]

$$\alpha = \frac{a_s[\mu_s - 0.1(\mu_p + \mu_d)]}{\mu_B} \tag{11}$$

with $a_s = 2.7$ MOe per $1\mu_B$ for ^{63,65}Cu. Evidently, the sign of these calculated coupling constants $\alpha(n)$ varies from site to site, as is observed in the NMR experiment in contrast to the simplified RKKY model.[6] Furthermore, the calculated α values (Table VI) are of the same order of magnitude as the experimental ones (Table V) although agreement is far from perfect.

A positive coupling constant is found for the Cu(3) site and for the Cu(1)/Cu(6) sites (which become inequivalent only below the phase transition from the orthorhombic to the monoclinic structure). On the other hand, negative coupling constants are obtained for the three other Cu sites, i.e., the Cu(4) and Cu(5) sites that have the smallest separation from their three Ce nearest neighbors, and the Cu(2) site—the only site that has four Ce neighbors and that is occupied by Au in $CeCu_5Au$. The alternation in sign of the transferred hyperfine field coupling constants, $\alpha(n)$, is not due to a variation in sign of the local conduction electron spin polarization. It is rather due to the relative weight of the partial s, p, and d contributions to the spin polarization. The partial s spin polarization acts at the nucleus via direct Fermi contact interaction with positive sign, whereas the p and d contributions act indirectly via core polarization with negative sign.[5] Therefore, $\alpha(n)$ in Eq. (11) may be negative even when all partial contributions to the spin polarization are positive. A small negative spin-polarization is only obtained for the d-like partial moments at the "squeezed" Cu(4) and Cu(5) sites (Table VI), but this is of negligible importance for the α value.

Actually, it is at first sight surprising that even the sites with positive α, Cu(1,6) and Cu(3), have a relatively large partial p occupation and barely larger partial s occupation (Table VI). These sites have the largest total number of electrons. This shows that it is important to distinguish between electron number, the spin polarization, and its orbital resolution in order to explain the transferred hyperfine coupling

TABLE VI. Results of energy-band calculation, imposing a Ce^{3+} $4f$ moment of $1\mu_B$. (Partial number n_i and magnetic moment μ_i of $i = s$-, p-, or d-like character in atomic spheres of the various structural sites of $CeCu_6$.)

	n_s	μ_s ($10^{-3}\mu_B$)	n_p	μ_p ($10^{-3}\mu_B$)	n_d	μ_d ($10^{-3}\mu_B$)	α (kOe/μ_B)
Ce	0.457	5.5	0.524	8.8	1.686	52.5	
Cu(1,6)	0.747	2.85	0.726	8.2	9.472	6.25	+3.80
Cu(2)	0.758	0.1	0.585	10.2	9.559	1.7	−2.94
Cu(3)	0.753	2.0	0.709	11.6	9.480	2.2	+1.67
Cu(4)	0.799	1.2	0.629	14.2	9.496	−0.3	−0.51
Cu(5)	0.768	0.8	0.671	10.9	9.475	−0.2	−0.73

constants of alternating sign and varying strength. We consider, for example, the Cu(3) site. The calculated value of $\alpha(3)=+1.67$ kOe/μ_B results from the partial compensation of a Fermi contact contribution of $\alpha_s(3)=+5.4$ kOe/μ_B due to the partial *s* polarization and a somewhat smaller negative non-*s* contribution. Thus, the experimentally observed sensitivity of the transferred field coupling constants $\alpha_i(n)$ to the details of the structural arrangements in the $CeCu_{6-x}Au_x$ isoelectronic pseudobinary compounds seems to originate from the peculiar situation that otherwise substantial *s* and non-*s* hyperfine contributions almost cancel for some Cu sites in these compounds. Because of the thus far neglected orbital contributions of the *p* and *d* electrons, anisotropy of the transferred field coupling constants has to be expected, and is actually observed.

B. Assignment of sites and EFGs

A comparison of the compiled calculated and measured NQR frequencies in Table II and the adopted assignment of Cu sites to measured NQR lines is self explanatory: The NQR frequencies increase from the Cu(2) site, which is occupied by Au in $CeCu_5Au$, over the Cu(1,6) sites, Cu(3) sites, and Cu(4) sites to the Cu(5) site, all numberings given in the orthorhombic denotation of $CeCu_6$. This general agreement is reassuring for the assignment of the NMR lines to the Cu sites. Here, the situation is even more complicated because the orientation of the local EFG tensor axes with respect to the *c* axis of the field oriented sample also has to be considered. Again the calculated spectra, shown in Fig. 5, allow for a clear-cut assignment of measured NMR lines to the Cu(*n*) sites. This assignment was applied as color code for the experimental results already presented in Fig. 4.

Taking the orientation of the single-crystal powder grains with their *c* direction parallel to the external field into account, the temperature-dependent NMR line positions can be described according to Sec. IV A, especially Eq. (7). The respective fits are included in Fig. 4. The relevant resulting parameters are discussed separately, i.e., the bare Knight shifts, $K_{0,c}$, in Sec. IV C 1, and the transferred field coupling constants, α_c, in Sec. IV C 2.

C. Hyperfine interaction

1. Bare Knight shift data

Only the *c*-axis values of the Knight shift, $K_{0,c}$ are accessible by the oriented powder analysis (Table IV). For $CeCu_6$, all Knight shifts are positive, indicative of dominating *s*-electron Fermi contact and orbital contribution of the conduction electrons. The site-specific variation seems to increase with *x*: Whereas for $CeCu_6$, there is at most 30% variation between the squeezed Cu(4) and Cu(5) sites and the other sites, the Knight shifts for Cu(1,6) and Cu(3) are larger, and those for the squeezed Cu(4) and Cu(5) sites lower (or even negative) for the antiferromagnet $CeCu_5Au$, revealing an increased *p* character for the latter sites. For the Cu(2) sites with the largest distance from the nearest Ce neighbors (occupied by Au for $CeCu_5Au$), the largest positive Knight shift $K_{0,c}$ is observed, in accordance with their smallest *p* contribution n_p in Table VI. Because of the low symmetry of the Cu sites and the presence of *p* electrons (Table VI), there will be a non-negligible anisotropy of $K_0(\theta,\phi)$. Thus, the individual experimental parameters $K_{0,c}(n)$ merit only a superficial discussion. We emphasize, nevertheless, that the average Knight shift $K_{0,c}$ for $CeCu_{6-x}Au_x$ in Table IV amounts to +0.262, +0.237, and +0.213%, for $x=0$, 0.1 and 1, quite close to the value of $K_0=+0.232\%$ observed in metallic copper.

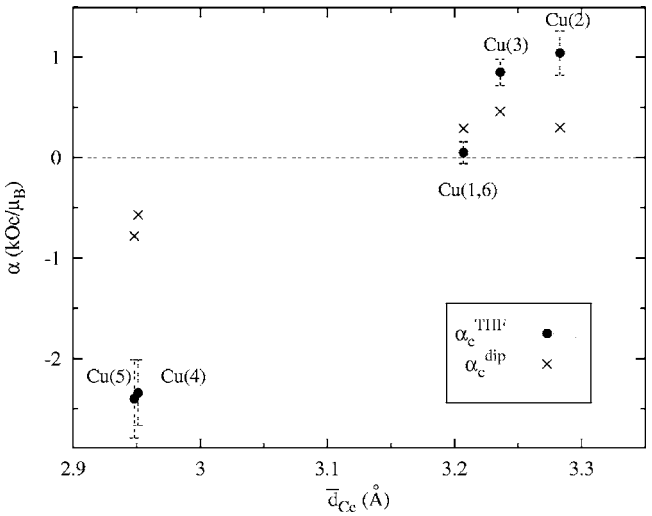

FIG. 6. Correlation between transferred field coupling constants, α_c^{THF} for the magnetically prefered *c* direction and average separation between Cu site and the 3 Ce nearest neighbors [four for Cu(2)] in $CeCu_6$. (The sum of the tabulated elemental radii amounts to $d=3.09$ Å.) The calculated classical dipole contribution, α_c^{dip}, is included for comparison [Eq. (2)].

2. Transferred hyperfine fields

The whole set of derived transferred hyperfine field coupling constants for *c* orientation is compiled in Table V. The varying sign was mentioned before. We start the discussion with the $CeCu_6$ data. The average value for all derived coupling constants is $\overline{\alpha_c}=-0.46$ kOe/μ_B and thus opposite to the sign of the orientation average derived in an early experimental report[10,11] with a polycrystalline powder sample at high temperatures (i.e., $\bar{\alpha}=+0.5$ kOe/μ_B) pointing to a pronounced anisotropy of α_i. After correction for the classical dipolar field contribution, the most relevant part, α_c^{THF}, is obtained, see right half of Table V. The negative sign for the "squeezed" Cu(4) and Cu(5) sites is in agreement with the numerical results in Table VI, just as with the positive sign for the Cu(3) and the Cu(1,6) sites. For the Cu(2) sites, the sign is interchanged. Figure 6 shows the apparent correlation between α_c^{THF}, the coupling constant of the hyperfine field, which is transferred from the Ce moments for their prefered *c* orientation to the Cu site in question by conduction electron or bonding electron polarization, and this site's average separation from the nearest (three or four) Ce neighbors.

For $x\neq 0$ in $CeCu_{6-x}Au_x$, the α_c^{THF} values show the same general behavior (Table V). Two observations merit further discussion: For the Cu(1,6) sites, $\alpha_c(1,6)$ changes sign for

$CeCu_5Au$. For these sites, p electron contribution seems to increase with increasing x. Second, the absolute value of the coupling constants $\alpha_c(n)$ is the smallest for $x=1$. However, inspecting the NMR line shift, e.g., for the Cu(4) site in Fig. 4 (second lowest frequency line), we see that the line shift actually is larger than for $x=0$. Thus, the small $\alpha_c(4)$ and $\alpha_c(5)$ for $x=1$ is due to the large $\chi_c(T)$ for $x=1$, or the comparably smaller Kondo-like shielding (λ) of the Ce^{3+} moments in this compound (Sec. IV A 1), compensating their action in Eq. (1) or (7). This indicates that the varying degree of Kondo-like shielding of the Ce moment in $CeCu_{6-x}Au_x$ does not influence the hyperfine field that is transfered from Ce^{3+} to the squeezed Cu(4) and Cu(5) sites, or the Cu(3) site, probably because different types of conduction or bonding electrons are concerned for Kondo-like shielding of the Ce^{3+} moment and for the transferred hyperfine interaction.

At a first glance, the transferred field coupling constants α_c^{THF} compiled in Table V may seem small: barely −2.5 kOe per $1\mu_B$ of Ce moment, not much more than the classical dipolar field. It has to be emphasized, however, that the dipolar field is proportional to $g\langle J_z\rangle$, whereas the spin-spin ($s-f$) exchange polarization is related to the spin part only, i.e., to $(g-1)\langle J_z\rangle$. For the $^2F_{5/2}$ ground state of Ce^{3+} due to the small Landé g factor of the $l-s$ spin orbit coupled $J=5/2$ configuration, $g=\frac{6}{7}$, the spin contribution is suppressed by the factor $(g-1)/g=-1/6$.

Remarkably, Table V shows, that the sign of α_c^{exp} of the various Cu sites for c-oriented Ce moments actually follows that of the classical dipolar field, suggesting the predominance of a pseudodipolar contribution. It has been clarified by Coqblin and Schrieffer[25] and Cornut and Coqblin[26] that for the Ce^{3+}-$4f^1$-configuration spin and orbit exchange scattering of the conduction electrons have to be taken into account. A strongly anisotropic Rudermann-Kittel interaction was thus predicted. The accompanying anisotropy of the transferred hyperfine interaction is difficult to substantiate experimentally for $CeCu_{6-x}Au_x$ due to the large single-ion magnetic anisotropy analyzed in Sec. IV A 1. Under these conditions, the anisotropy of the paramagnetic NMR line shift, Eq. (7) is dominated by the anisotropy of the magnetic susceptibility $\chi_i^{\mathrm{mol}}(T)$ (Fig. 2). The anisotropy of $\alpha_i^{\mathrm{THF}}(n)$, inspite of being difficult to assess experimentally, is of particular importance for the understanding of the electronic structure of these intermetallic compounds, however. Fortunately, some Cu-NMR lines for well-defined orientations of the magnetic field different from the arrangement with field parallel to the c axis exclusively accessible for the oriented single-crystal powder samples have been observed in our earlier $CeCu_6$ polycrystalline powder NMR attempts.[6] They could now be assigned to individual sites, Cu(n), and field orientations by means of calculated NMR spectra based on the electric field gradient information, and by comparison to the experimental $\chi_a, \chi_b, \chi_c(T)$ data (Fig. 2). Table V includes the parameter α_a^{exp} thus obtained for the squeezed Cu(5) site. The a orientation is extracted from Figs. 2 and 5 of Ref. 6 (In Fig. 2, the respective line is termed line 6 and is found at 77.2 MHz; the correlation of its position with the susceptibility χ_a is shown in the right panel of Fig. 5 of Ref. 6), taking into account that the edge singularity of the electric field gradient tensor of the Cu(5) site is reached at an angle of 13° with respect to the a axis in the a-c plane. $\alpha_a(5)$ has the opposite sign to $\alpha_c(5)$. The anisotropic contribution of $\alpha(5)$ is thus evidently larger than the isotropic one. Separating a pseudodipolar contribution (f^{pd}) from the α_i^{THF} part of Eq. (2), i.e.,

$$\alpha_i(n) = [1 + f^{pd}(n)]\alpha_i^{\mathrm{dip}}(n) + \alpha_{\mathrm{iso}}^{\mathrm{THF}}(n) \qquad (12)$$

we derive $f^{pd}=4.44$ and $\alpha_{\mathrm{iso}}^{\mathrm{THF}}=+1.065$ kOe/μ_B for the Cu(5) site. Thus, this observation supports a highly anisotropic spin and orbital exchange scattering mechanism as introduced for the Ce-$4f^1$ configuration by Coqblin and Schrieffer[25] and Cornut and Coqblin.[26]

V. CONCLUSIONS

The pseudobinary intermetallic compounds $CeCu_{6-x}Au_x$ received considerable interest recently because $CeCu_6$ is one of the best-known heavy-fermion paramagnets, $CeCu_5Au$ is a heavy-fermion antiferromagnet with $T_N=2.3$ K and $CeCu_{5.9}Au_{0.1}$, with $T_N \to 0$, showed signatures of non-Fermi liquid behavior. To allow more significant NMR contributions for this rather active field of research in the future, we unraveled their magnetic resonance spectra of ^{63,65}Cu in the temperature range, 5–100 K. We established a conclusive assignment of the 12 ^{63,65}Cu NQR lines and the 24 or more resolved ^{63,65}Cu NMR lines (for c-oriented external field) to the various inequivalent Cu sites in the heavy-fermion compounds $CeCu_{6-x}Au_x$ ($0 \leqslant x \leqslant 1$), based on appropriate, sufficiently accurate self-consistent electronic structure calculations. Our Ce^{3+} crystal field analysis, based on the single-crystal magnetic susceptibility, indicates that (Kondo-like) shielding of the Ce moment is less pronounced for $CeCu_5Au$ than for $CeCu_6$. All site specific Cu bare Knight shifts $K_{0,c}(n)$ in $CeCu_6$ are positive, similar in value to elemental Cu, and do, at most, differ by 30%. For the Cu(4) and Cu(5) sites that are squeezed between Ce moments, the Knight shift tends to negative values (more p-like character) for $CeCu_5Au$, in contrast to the more spacious Cu(1,6) and Cu(3) sites. The observed substantial paramagnetic NMR line shifts for orientation of the magnetic field parallel to the preferred c direction have different signs, and they are, in part, more than a factor of 5 larger than an early published average value.[10,11] Only for the Cu(1) and Cu(6) sites, (that become inequivalent for $CeCu_6$ in the low-temperature monoclinic phase) the classical dipolar field predominates in the total hyperfine field that is transferred from the Ce moments to the Cu(1,6) sites. At all other Cu sites the contribution α^{THF} originating from polarized conduction or bonding electrons surpassed the classical dipolar field, up to a factor of 4, even when contributing with the same sign. There seems to exist a simple correlation between strength and sign of the transferred hyperfine field for the c orientation and average separation to the three or four nearest Ce neighbors: large negative values are observed for close neighbors, positive values for distant neighbors. Remember that the average Ce-Cu separation for the close neighbors is smaller than the sum of the tabulated elemental radii, which would be $r_{Cu}+r_{Ce}=3.09$ Å,[6] and that for the

light rare earth ion Ce^{3+} the negative sign of α^{THF} means ferromagnetic orientation of the local field with respect to the $4f$ electron spin. The peculiarity observed for the heavy fermion compounds $CeCu_{6-x}Au_x$ $(0 \leqslant x \leqslant 1)$, in distinction to "normal" rare-earth intermetallic compounds,[5] is the predominance of the p-like contribution of the electron polarization at the Cu sites, i.e., μ_p/μ_s in the average is >10 in Table VI. Thus, the negative non-s contribution almost cancels or even outweighs the positive s-like contribution of the transferred field coupling constant $\alpha^{THF}(n)$ of the various Cu sites. The paramagnetic NMR line shifts follow, in general, the intrinsic magnetic susceptibility, that can be calculated from the Ce^{3+} crystal field splitting, corrected for Kondo-like shielding. However, the experimentally observed macroscopic single-crystal susceptibility $\chi_c(T)$ exhibits at intermediate temperatures a somewhat stronger decrease with increasing temperature, questioning the assumption of a temperature-independent λ value. Furthermore, the x-dependent degree of Kondo-like shielding of the Ce^{3+} moment, which is observed in the static magnetic susceptibility, seems of minor influence for the hyperfine field that is transferred to the Cu sites, at least for the Cu(3), Cu(4), and Cu(5) sites. For the Cu(5) site (with the closest separation to its Ce neighbors), a predominatly anisotropic transferred field coupling constant has been derived. This could not be explained by a simple spin-spin sf exchange interaction, but it proves the impact of spin and orbit exchange scattering for the Ce^{3+}-$4f^1$ configuration, as introduced long ago by Coqblin and Schrieffer.[25]

In summary, the characteristic of the heavy-fermion compounds $CeCu_{6-x}Au_x$, $0 \leqslant x \leqslant 1$ is that the contribution of exchange polarized p-like Cu electrons is by a factor of at least 10 larger than in ordinary rare-earth intermetallic compounds. Kondo-like shielding of the Ce moments is the weakest for the heavy-fermion antiferromagnet $CeCu_5Au$ $(x=1)$. No specific feature is observed in this NMR analysis at temperatures $T>5$ K for the non-Fermi-liquid system with $x \approx 0.1$. These detailed results should be useful for further, even more relevant NMR/NQR studies of the peculiarities of the heavy-fermion behavior in $CeCu_{6-x}Au_x$ at temperatures below 5 K.

ACKNOWLEDGMENTS

We thank H. v. Löhneysen and O. Stockert for the samples and for discussions. This research was supported by the Deutsche Forschungsgemeinschaft within the Project Do 181/11.

[1] H. v. Löhneysen, J. Magn. Magn. Mater. **200**, 532 (1999).
[2] H. v. Löhneysen, T. Pietrus, G. Portisch, H. G. Schlager, A. Schröder, M. Sieck, and T. Trappmann, Phys. Rev. Lett. **72**, 3262 (1994).
[3] J. Rossat-Mignod, L. P. Regnault, J. L. Jacoud, C. Vetter, P. Lejay, J. Flouquet, E. Walker, D. Jaccard, and A. Amato, J. Magn. Magn. Mater. **76-77**, 376 (1988).
[4] K. Yosida, Phys. Rev. **106**, 893 (1957).
[5] E. Dormann, in: *Handbook on the Physics and Chemistry of Rare Earths*, edited by K. A. Geschneidner, Jr., and L. Eyring (Elsevier/North-Holland, Amsterdam, 1991), Vol. 14, p. 63, and references therein.
[6] M. Winkelmann, G. Fischer, B. Pilawa, and E. Dormann, Eur. Phys. J. B **26**, 199 (2002).
[7] P. Pyykkö, Mol. Phys. **99**, 1617 (2001).
[8] D. T. Cromer, A. C. Larson, and R. B. Roof, Jr., Acta Crystallogr. **13**, 913 (1960).
[9] M. Ruck, G. Portisch, H. G. Schlager, M. Sieck, and H. v. Löhneysen, Acta Crystallogr., Sect. B: Struct. Sci. **B49**, 936 (1993).
[10] I. Pop, M. Coldea, and V. Niculescu, Czech. J. Phys., Sect. B **24**, 1398 (1974).
[11] M. Coldea and I. Pop, Acta Phys. Pol. A **A48**, 359 (1975).
[12] T. Shimizu, M. Takigawa, H. Yasuoka, Y. Onuki, and T. Komatsubara, J. Phys. Soc. Jpn. **54**, 470 (1985).
[13] K. Kumagai, I. Watanabe, H. Nakajima, Y. Onuki, and T. Komatsubara, Jpn. J. Appl. Phys., Suppl. **26**(3), 533 (1987).
[14] Y. Kitaoka, K. Fujiwara, Y. Kohori, K. Asayama, Y. Onuki, and T. Komatsubara, J. Phys. Soc. Jpn. **54**, 3686 (1985).
[15] K. Kumagai, H. Aoki, H. Nakajima, Y. Onuki, and T. Komatsubara, Jpn. J. Appl. Phys., Suppl. **26**(3), 531 (1987).
[16] L. Pollack, M. J. R. Hoch, C. Jin, E. N. Smith, J. M. Parpia, D. L. Hawthorne, D. A. Geller, D. M. Lee, R. C. Richardson, D. G. Hinks, and E. Bucher, Phys. Rev. B **52**, R15707 (1995).
[17] T. Omuta, K. Fujiwara, J. Takeuchi, Y. Kohori, and T. Kohara, Physica B **259–261**, 378 (1999).
[18] R. E. Walstedt, H. Kojima, N. Butch, and N. Bernhoeft, Phys. Rev. Lett. **90**, 067601 (2003).
[19] P. Carretta, M. Giovannini, M. Horvatić, N. Papinutto, and A. Rigamonti, Phys. Rev. B **68**, 220404(R) (2003).
[20] P. Blaha, K. Schwarz, and P. H. Dederichs, Phys. Rev. B **37**, 2792 (1988).
[21] P. Blaha, K. Schwarz, G. K. H. Madsen, D. Kvasnicka, and J. Luitz, *WIEN2k, An augmented Plane Wave+Local Orbitals Program for Calculating Crystal Properties* (Karlheinz Schwarz, Techn. Universtät Wien, Austria, 2001).
[22] T. J. Bastow, M. I. Burgar, and C. Maunders, Solid State Commun. **122**, 629 (2002).
[23] E. Dormann, *Hyperfeinfelder in Magnetisch Geordneten, Intermetallischen Seltenerdverbindungen: Kern-Spin Echo Untersuchungen* (Habilitationsschrift, Technische Hochschule Darmstadt, 1975).
[24] E. Dormann, M. Huck, and K. H. J. Buschow, Z. Phys. B **27**, 141 (1977).
[25] B. Coqblin and J. R. Schrieffer, Phys. Rev. **185**, 847 (1969).
[26] B. Cornut and B. Coqblin, Phys. Rev. B **B5**, 4541 (1972).
[27] E. Kerscher, Diplomarbeit, Universität Karlsruhe, 2000.
[28] E. Kerscher, M. T. Kelemen, K. H. Diefenbach, O. Stockert, H. v. Löhneysen, and E. Dormann, Eur. Phys. J. B **19**, 241 (2001).
[29] M. Winkelmann, Diplomarbeit, Universität Karlsruhe, 2001.
[30] K. H. Diefenbach, Diplomarbeit, Universität Karlsruhe, 1998.
[31] M. Winkelmann, G. Fischer, and E. Dormann, J. Magn. Magn. Mater. **272–276**, e125 (2004).

[32] Y. Onuki, Y. Shimizu, and T. Komatsubara, J. Phys. Soc. Jpn. **54**, 304 (1985).
[33] S. Takayanagi, Y. Onuki, and T. Komatsubara, J. Phys. Soc. Jpn. **55**, 2384 (1986).
[34] B. Stroka, A. Schröder, T. Trappmann, H. v. Löhneysen, M. Loewenhaupt, and A. Severing, Z. Phys. B: Condens. Matter **90**, 155 (1993).
[35] S. P. Strong and A. J. Millis, Phys. Rev. B **50**, 12611 (1994).
[36] T. P. Das and E. L. Hahn, *Solid State Physics*, edited by F. Seitz and D. Turnbull (Academic Press, New York, 1958), Suppl. 1.
[37] G. C. Carter, L. H. Bennett, and D. J. Kahan, in *Physics in Material Science*, edited by B. Chalmers, J. W. Christian, and T. B. Massalski (Pergamon Press, London, 1977), Vol. 20.
[38] O. K. Andersen, Phys. Rev. B **12**, 3060 (1975).
[39] O. K. Andersen and O. Jepsen, Phys. Rev. Lett. **53**, 2571 (1984).
[40] U. von Barth and L. Hedin, J. Phys. C **5**, 1629 (1972).
[41] P. Hohenberg and W. Kohn, Phys. Rev. **136**, B864 (1964).
[42] W. Kohn and P. Hohenberg, Phys. Rev. **140**, A1133 (1965).
[43] M. S. S. Brooks, T. Gasche, S. Auluck, L. Nordström, L. Severin, J. Trygg, and B. Johansson, J. Appl. Phys. **70**, 5972 (1991).